Multiplexed stimulated emission depletion nanoscopy (mSTED) for 5-color live-cell long-term imaging of organelle interactome

Yuran Huang, Zhimin Zhang, Wenli Tao, Yunfei Wei, Liang Xu, Wenwen Gong, Jiaqiang Zhou, Liangcai Cao, Yong Liu, Yubing Han, Cuifang Kuang and Xu Liu

---

Related articles

3D imaging lipidometry in single cell by in-flow holographic tomography
Daniele Pirone, Daniele Sirico, Lisa Miccio, Vittorio Bianco, Martina Mugnano, Danila del Giudice, Gianandrea Pasquinelli, Sabrina Valente, Silvia Lemma, Luisa Iommarini, Ivana Kurelac, Pasquale Memmolo, Pietro Ferraro
Opto-Electronic Advances   2023 **6**, 220048   doi: 10.29026/oea.2023.220048

Improved spatiotemporal resolution of anti-scattering super-resolution label-free microscopy via synthetic wave 3D metalens imaging
Yuting Xiao, Lianwei Chen, Mingbo Pu, Mingfeng Xu, Qi Zhang, Yinghui Guo, Tianqu Chen, Xiangang Luo
Opto-Electronic Science   2023 **2**, 230037   doi: 10.29026/oes.2023.230037

Speckle structured illumination endoscopy with enhanced resolution at wide field of view and depth of field
Elizabeth Abraham, Junxiao Zhou, Zhaowei Liu
Opto-Electronic Advances   2023 **6**, 220163   doi: 10.29026/oea.2023.220163

More related article in Opto-Electronic Journals Group website

Multiplexed stimulated emission depletion nanoscopy (mSTED) for 5-color live-cell long-term imaging of organelle interactome

Yuran Huang[1†], Zhimin Zhang[1,2†], Wenli Tao[1†], Yunfei Wei[3], Liang Xu[1], Wenwen Gong[1], Jiaqiang Zhou[4], Liangcai Cao[5], Yong Liu[6], Yubing Han[1,3]*, Cuifang Kuang[1,2,7]* and Xu Liu[1,2]

Stimulated emission depletion microscopy (STED) holds great potential in biological science applications, especially in studying nanoscale subcellular structures. However, multi-color STED imaging in live-cell remains challenging due to the limited excitation wavelengths and large amount of laser radiation. Here, we develop a multiplexed live-cell STED method to observe more structures simultaneously with limited photo-bleaching and photo-cytotoxicity. By separating live-cell fluorescent probes with similar spectral properties using phasor analysis, our method enables five-color live-cell STED imaging and reveals long-term interactions between different subcellular structures. The results here provide an avenue for understanding the complex and delicate interactome of subcellular structures in live-cell.

Keywords: optical nanoscopy; phasor analysis; multicolor live cell imaging

Introduction

An increasing body of research indicates that the subcellular structures within cells establish an intricate network of interactions to facilitate crucial physiological functions[1,2]. Over the past two decades, super-resolution fluorescence microscopy (SR) has continued to change the perception of the power of fluorescence microscopy, pushing the resolution of remote optical microscopy to the order of tens of nanometers, allowing the study of nanoscale intracellular organelles under the diffraction limit[3–12]. However, the interactions between the ultrafine subcellular structures are both systematic and complex in living cells, making it still challenging to analyze their structure, dynamics, and functions under physiological and pathological conditions using multi-color super-resolution imaging[1,2].

[1]State Key Laboratory of Extreme Photonics and Instrumentation, College of Optical Science and Engineering, Zhejiang University, Hangzhou 310027, China; [2]Research Center for Intelligent Chips and Devices, Zhejiang Lab, Hangzhou 311121, China; [3]Wuhan National Laboratory for Optoelectronics, Huazhong University of Science and Technology, Wuhan 430074, China; [4]Department of Endocrinology and Metabolism, Sir Run Run Shaw Hospital, Zhejiang University School of Medicine, Hangzhou 310016, China; [5]Department of Precision Instruments, Tsinghua University, Beijing 100084, China; [6]College of electronics and information engineering, Shanghai University of Electrical Power, Shanghai 200090, China; [7]ZJU-Hangzhou Global Scientific and Technological Innovation Center, Hangzhou 311200, China.
†These authors contributed equally to this work.
*Correspondence: YB Han, E-mail: hanyubing@zju.edu.cn; CF Kuang, E-mail: cfkuang@zju.edu.cn
Received: 17 February 2024; Accepted: 11 May 2024; Published online: 5 July 2024

Stimulated emission depletion microscopy (STED) is one of the leading techniques beyond the diffraction limit[4,13], and it ensures minimal artifacts by its immediate super-resolution microscopic properties without post-processing[14,15]. In the last decade, the need to study the interactions between subcellular structures has led to an increasing interest and application of multicolor live-cell STED, most conventionally achieved by using multiple excitation-depletion beam pairs[16,17]. However, increasing the number of depletion beams not only makes the system more complex and dramatically increases the construction cost, but also increases the likelihood of photobleaching and more severe photo-cytotoxicity, which is not conducive to live-cell imaging. On the other hand, the use of a single depletion beam along with multiple excitation beams limits the range of available excitation wavelengths, and dividing the restricted band into multiple densely arranged spectral channels and reducing crosstalk between them poses a significant challenge[18]. Currently, with the help of long Stokes-shifted dyes, two to three color STED is the most commonly achieved with this method[19−21]. In addition, other researchers have used fluorescence spectral differentiation[18,22,23] or light-switching properties of fluorescent groups[24] to achieve multi-color STED imaging.

Apart from the methods mentioned above to achieve multi-color imaging, a rising method to achieve structure segmentation is to exploit the natural difference of the fluorescence lifetime[25−28]. Conventional fitting-based fluorescence lifetime imaging methods, when applied in multi-color imaging, require the simultaneous fitting of multiple variables on a pixel-by-pixel basis, which is time-consuming and requires a lot of photons[29]. In contrast, phasor approach solves these problems by converting time-domain analysis into phase-domain analysis. It has proven to be an excellent tool for lifetime-based multicolor imaging[30−32] and has been extended to address multiple separations in both lifetime and spectral domains[33,34].

A number of researchers have used phasor approach in STED microscopy to analyze fluorescence lifetime differences between multiple labels[29,35−37]. However, these methods have primarily been applied to fixed cells. The difficulties in i) screening out live-cell probes with brightness and anti-bleaching properties suitable for STED imaging, ii) simultaneously labeling multiple subcellular structures in living cells, and iii) separating different fluorescent probes in the same spectral channel

using proper phasor plot analysis hindered its application in live-cell STED imaging. Due to these challenges, biologists currently face a lack of effective methods for studying the dynamics and function of subcellular structures using STED microscopy, as the interactions of four or more subcellular structures are difficult to observe. Hence, arises the need to develop multi-color STED microscopy for live-cell imaging.

Here, we propose a live-cell multi-color STED method (mSTED) that takes advantage of clustered proportional partitioning of fluorescence lifetime phasor analysis and multiple labeling of subcellular structures with live-cell fluorescent probes. By combining the phase-distribution properties of fluorescence with live-cell STED microscopy, we show in this work long-term 5-color live-cell super-resolution imaging with limited photobleaching was achieved in mSTED, enlightening research on biological topics such as subcellular structural interactome.

Methods

Setup of mSTED

In traditional STED, multiple staining of fluorescent probes with similar excitation and emission spectra may lead to confusion in recognizing subcellular structures when using the same excitation laser. While fluorescence lifetime is the inherent property of specific fluorophores, different lifetime values can be used to assign the identity of the probes, if this value can be acquired in imaging (Fig. 1(a)). We implemented this method in a mSTED instrument and investigated the fluorescence lifetime separation of live-cell fluorescent probes in the same spectral channel.

mSTED can be implemented with a few modifications to a common STED microscope. As depicted Supplementary information Fig. S1, we constructed a system that consisted of two pulsed excitation beams (Picoquant LDH series) commonly used at wavelengths of 560 nm and 640 nm, along with a high-power depletion beam (Onefive GmbH Katana-08 HP) at a wavelength of 775 nm. where the depletion beam is vortex phase modulated and focused by the objective lens (Nikon CFI Plan Apochromat DM Lambda 100X Oil) to form a donut-shaped spot, thus suppressing fluorescence emission from fluorescent molecules located at the periphery of the excitation spot. The remaining fluorescence is detected by the avalanche photodiode (Excelitas SPCM-AQRH-TR series) after passing through the dichroic
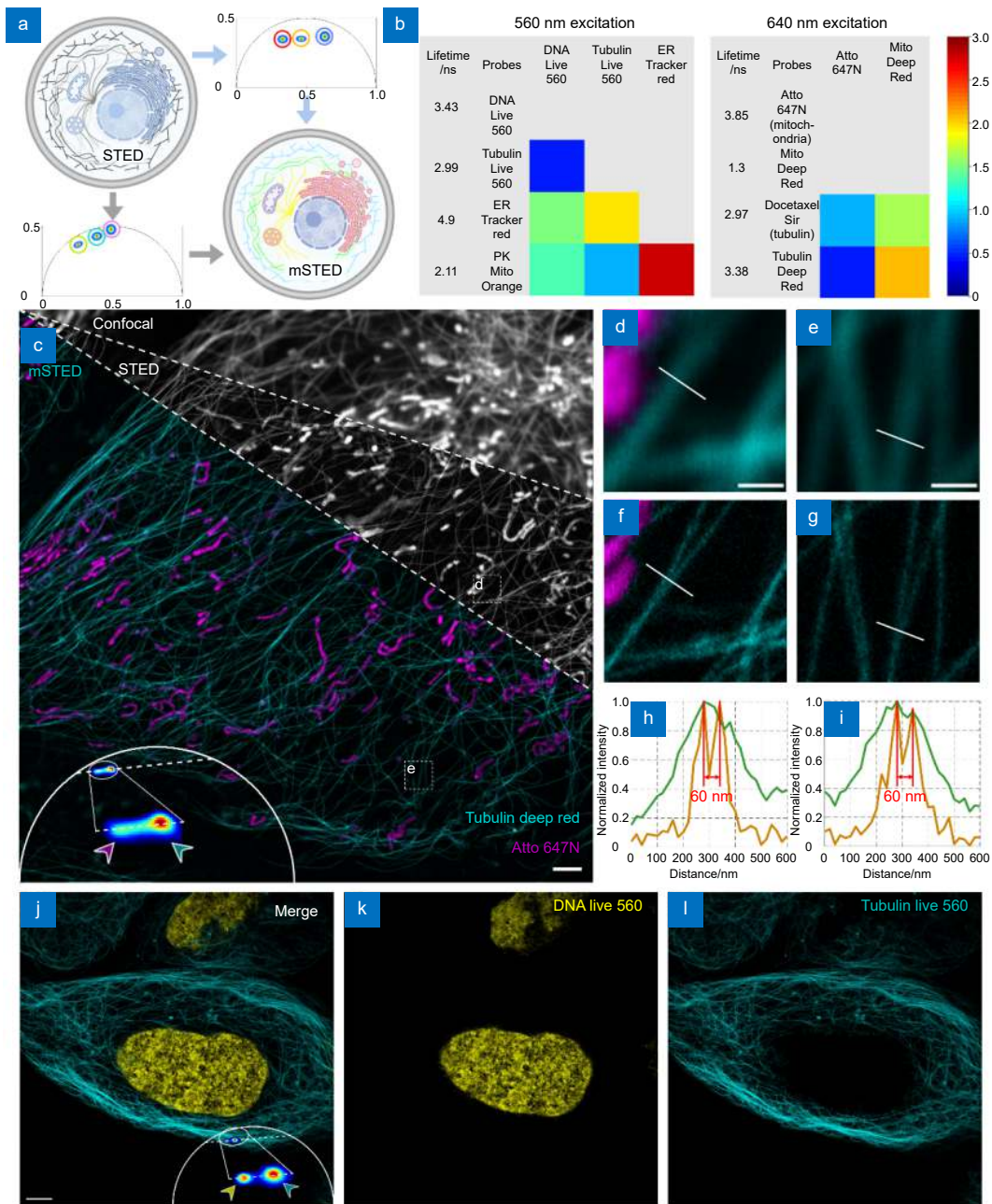
Fig. 1 | mSTED structure identification. (**a**) Schematic diagram of fluorescence lifetime multiplexing, where spectral multiplexing contains only a limited number of spectral channels, whereas lifetime multiplexing by phasor analysis allows simultaneous observation of all the different structures. (**b**) Fluorescent probe selection strategy, four live-cell STED probes were selected at 560 nm and 640 nm excitation wavelength each and the difference in fluorescence lifetimes between them was measured. (**c**) Comparison of mSTED with confocal and STED, the greyscale image represents the intensity map obtained by Confocal and STED imaging, while the colored image demonstrates that mSTED can identify mitochondria and microtubules after phase analysis. The phasor points are projected onto the fitted line and further classified, ultimately leading to the segmentation of the intensity image. Live U2OS cells were labeled with Atto 647N (magenta; mitochondria) and Tubulin Deep Red (cyan; microtubules). The two structures were simultaneously excited by a beam at a wavelength of 640 nm. The clusters indicated by magenta and cyan arrows in the phasor plot correspond to mitochondria and microtubules, respectively. (**d**–**g**) Comparison of mSTED imaging versus confocal imaging of segmented mitochondria and microtubules, corresponding to the regions marked by the white boxes in (c). (**h**, **i**) Line profiles along the dotted lines in (**f**,g) which show that STED is able to separate two microtubules in close proximity, revealing details unobservable by confocal images. The presence of sharp peaks in the profile suggests that the mSTED image exhibits a resolution of 60 nm. (**j**–**l**) Identification of DNA and microtubules using mSTED in the 560-nm excitation channel. Live U2OS cells were labeled with DNA Live 560 (yellow; DNA) and Tubulin Live 560 (cyan; microtubules). Scale bars: (c) 2 μm; (d, e) 500 nm; (j) 5 μm.

mirror. The introduction of the depletion beam will lead to a decrease in the number of fluorescent photons and a shortening of the fluorescence lifetime, making it difficult to separate different structures. To address this shortcoming, we added an acousto-optic modulator to the depletion beam path, which enables the depletion beam to switch on and off line by line, and to use the fluorescence signals obtained when the depletion beam is turned off as the basis for separating different structures. In STED imaging based on intensity identity, the fluorescence signals are fed into the data acquisition card to be counted; whereas in our mSTED, time-correlated single-photon counting techniques (TCSPC, Siminics FT1080) is used to detect the time difference between the acquired fluorescence signal and the excitation pulse signal. By counting the time difference pixel by pixel, the fluorescence decay can be obtained.

Phasor analysis

Phasor analysis was introduced to convert fluorescence decays into color-mapped images where different colors represent different fluorophores[30]. Instead of a complex and time-consuming fitting process, this analysis transforms each decay into two coordinates in a polar plot. Thus, the position of each point in the phasor plot represents the fluorescence lifetime of each pixel. To correctly calculate the phasor plot, only two additional parameters are needed: the temporal resolution of the TCSPC and the angular frequency of the excitation pulse. Further consideration of the instrument response function (IRF) helps to obtain a more accurate phasor plot. Detailed method for acquiring fluorescence decay, phasor analysis and mitigating the effects of IRF are outlined in Supplementary information Section 1.

When multiple fluorescent probes overlap each other, the fluorescence decay of some pixels may have multiple contributions. According to the phasor theorem, these pixels correspond to phasor points located in the middle of multiple phasor clusters. To separate the overlapping fluorescent probes, we projected these phasor points onto the line obtained from the fitting, and proportionally allocated the number of photons from the corresponding pixel into the two structures based on the reciprocal of their distances to the respective phasor clusters, thus generating mSTED images. Isolated points caused by noise and microenvironmental variations are eliminated to suppress crosstalk between structures. In Supplementary information Fig. S8, we provide an illustrative exam-

ple of how we separated mitochondria and microtubules when they overlapped each other. The implementation of this process is described in Supplementary information Section 2.

Fluorescent probe selection

In monochromatic imaging, phasor points tend to form distinct clusters; whereas in mSTED, phasor plot comprises multiple clusters. If the selected fluorescent probes have similar lifetimes, the phasor clusters will exhibit significant overlap. Hence, it is crucial to choose fluorescent probes based on their distinct lifetimes. The fluorescence lifetime of a series of commonly-used fluorescent probes for live-cell imaging was first measured, and their difference values were calculated. Two- and multi-color labeling experiments were subsequently performed to assess the viability of various probe combinations. Our evaluation focused on detecting any potential crosstalk between individual structures during multi-color imaging. Based on the empirical results obtained, in Fig. 1(b), we list a number of feasible probes combinations that can ensure reliable separation of different structures for accurate and precise analysis. Probe dosages and labeling methods are described in Supplementary information Section 3. However, it is worth noting that when the state or microenvironment (pH, viscosity, etc)[38] of the cell is unstable, variation in fluorescence lifetimes may result in the original difference in lifetimes being insufficient for proper separation of structures, e.g., in Supplementary information Fig. S6, a portion of the probe labeled with lysosomes has the same fluorescence lifetime as the probe labeled with DNA. At this point combinations of probes with greater differences in lifetime are required.

Results and discussion

Structure identification in live-cell STED based on phasor analysis

First we demonstrated the ability of mSTED to separate two different structures. However, this method can also be employed for multi-color imaging of structures with sufficiently distinct fluorescence lifetimes. In Fig. 1(c), Tubulin Deep Red and Atto 647N were used to label microtubules and mitochondria in U2OS cells. Due to the overlapping excitation and emission spectra of these two probes, segmentation in STED imaging based solely on intensity was very difficult. Nevertheless, by analyzing the lifetime information, we were able to assign different

colors to pixels corresponding to distinct clusters in the phasor plot, effectively separating different biological structures. We also observed centrosomes with hollow structures (Fig. S9). The fluorescence lifetime of the centrosome region was not disturbed, allowing it to be distinguished from that of mitochondria. A similar outcome was achieved at a wavelength of 560 nm in Fig. 1(j–l), where the significant difference in lifetime between DNA Live 560 and Tubulin Live 560 resulted in the appearance of two distinct clusters in the phasor plot, corresponding to DNA (Fig. 1(k)) and microtubules (Fig. 1(l)). To verify the accuracy of the segmentation results, we labeled mitochondria (Tubulin Deep Red) and microtubules (Mito Deep Red) in the 640-nm excitation channel, while simultaneously labeling mitochondria (Mito Tracker Red) in the 560-nm excitation channel as ground truth. Supplementary information Fig. S4 shows that mitochondria have a consistent distribution in the 560-nm excitation channel and in the 640-nm excitation channel where mSTED imaging was performed, with a crosstalk of only 4%, validating the reliability of mSTED results.

Although the lifetime-based multiplexing method remains applicable in confocal microscopy, its limited resolution can hinder the observation of subtle cellular activities. In this study, we present the capability of mSTED to enable simultaneous super-diffraction limited imaging of multiple structures within living cells. Fig. 1(d–g) illustrates a comparison between the imaging effects of STED and confocal microscopy on isolated mitochondria and microtubules, corresponding to the regions indicated by the arrows in Fig. 1(c). The STED images reveal finer details of the microtubules and mitochondria, effectively separating the structures that are confounded in the confocal microscope. A more visually striking comparison is depicted in Fig. 1(h–i), where mSTED produces sharp peaks that are not visible in confocal microscopy. Since the resolution of STED imaging strictly depends on the power of excitation and depletion laser, we achieved the highest resolution of 60 nm by using Tubulin Deep Red and Atto 647N probe with 640-nm excitation laser (power density of 3.1 kW/cm² for excitation laser and 26 MW/cm² for depletion laser) and 90 nm using DNA Live 560 and Tubulin Live 560 with 560-nm excitation laser (Fig. S5, power density of 7.5 kW/cm² for excitation laser and 32 MW/cm² for depletion laser). To better illustrate the resolution of mSTED, we also statistically analyzed the diameters of the micro-

tubules in Fig. 1(c) and obtained a full-width half-maximum of 56 ± 5.8 nm, which can be viewed in detail in Supplementary information Fig. S11. The resolution of mSTED under lower depletion intensity is also addressed in Supplementary information Fig. S12 and Supplementary information Section 4.

Reduced photo-bleaching and photo-cytotoxicity in mSTED

To verify the performance of mSTED in photo-bleaching and photo-cytotoxicity, we performed dual-staining of live-cell and observed the samples with both traditional dual-color STED and our mSTED imaging. The mitochondrial shapes were chosen as one of the key indications since mitochondria are very sensitive to photo-cytotoxicity[39]. We also focused on the fluorescence intensity after long-term imaging to compare the photo-bleaching level of the two methods.

In the experiment, we controlled the variables by setting the cell types, labeling dosage and laser power of both excitation and depletion lasers to be the same. Additionally, the dwell time will also significantly affect photo-bleaching and photo-cytotoxicity. Both conventional two-color STED and mSTED were set to a dwell time of 10 μs. Consequently, it took 13.16 s and 6.58 s to acquire a single frame of conventional two-color STED image and mSTED image, respectively. 6.58 s also represents the highest temporal resolution in the mSTED images covered in the full paper. Utilizing the reduced photon counting requirements of phase analysis, mSTED imaging only necessitates a dwell time of up to 20 μs. This results in a total single-frame imaging time in the order of seconds to tens of seconds, depending on the field-of-view.

In traditional dual-color STED, two pairs of excitation-depletion lasers were implemented to excite and deplete the two probes from different spectra separately, resulting in significant photo-bleaching and photo-cytotoxicity (Fig. 2(a) and 2(c)). We used Tubulin Deep Red and Mito Tracker Red to stain microtubules and mitochondria in live-cell and tested their performance in traditional dual-color STED. During the whole imaging duration for ~11 min, the two probes in traditional dual-color STED were gradually bleached to invisible (Tubulin Deep Red signal: 13.4% remained; Fig. 2(d)). At the same time, the mitochondria turned into swollen and round shapes, indicating severe photo-cytotoxicity (white arrows in Fig. 2(c)). In contrast, for dual-color
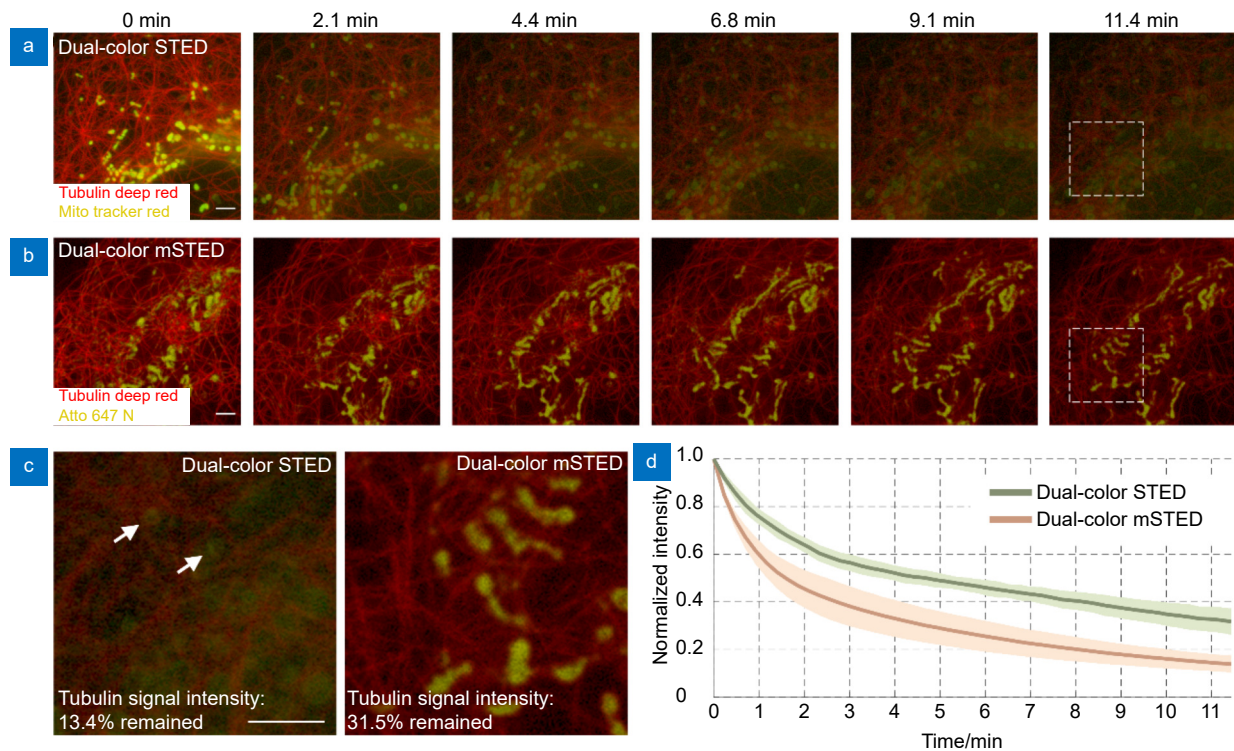
Fig. 2 | Photo-bleaching and photo-cytotoxicity of mSTED. (**a**) Traditional dual-color STED imaging of mitochondria and microtubules in live-cell, labeled with Tubulin Deep Red (red; microtubules) and Mito Tracker Red (yellow; mitochondria) and excited alternately with two beams at wavelengths of 640 nm and 561 nm. (**b**) Dual-color mSTED imaging of mitochondria and microtubules in live-cell, labeled with Tubulin Deep Red (red; microtubules) and Mito Tracker Red (yellow; mitochondria) and excited simultaneously with a beam at wavelength 640 nm. For the time-lapse imaging, the acquire time was 10 µs for each single dual-color image in traditional STED and 10 µs for dual-color mSTED, and the interval time between each image was set as 14 s. Representative frames were displayed. (**c**) magnified views of the white-boxed regions in (a, b). (**d**) Photo-bleaching curves of the same probe Tubulin Deep Red under dual-color STED and mSTED imaging (mean value ± standard deviation). Scale bars: 2 µm.

mSTED imaging, the probes from the same spectra need only one pair of excitation-depletion laser, thus halving the introduction of laser dose (Fig. 2(b) and 2(c)). In mSTED mode, Mito Tracker Red was substituted by At-to 647N as a mitochondrial marker to fit the 640-nm excitation laser. After imaging for 11 min, the structures of both mitochondria and microtubules were still visible, and 31.5% of the microtubule signal remained (Fig. 2(b–d)). There was no significant swelling of the mitochondria, indicating reduced photo-cytotoxicity. Taken together, the above results suggest an evident reduction in photo-bleaching and photo-cytotoxicity in dual-color mSTED than traditional STED.

Multi-color live-cell mSTED with single excitation beam

Multi-color imaging is of essence to discover the interactions between subcellular structures during physiological and pathological activities. The multi-color feasibility of live-cell mSTED using only one excitation laser beam was investigated (Fig. 3(a–c)). Three dyes (i.e., DNA Live 560, Tubulin Live 560, PK Mito Orange) excited at 560 nm were successfully separated following proper segmentation (Fig. 3(a)). Interactions between the nuclear, microtubules, and mitochondria at the same time were revealed. The result showed that microtubules form a denser network around the nucleus than in the periphery (white arrows in Fig. 3(b)), and some mitochondria moving along microtubules turned to another direction at the microtubule intersections, forming a bending angle (yellow arrows in Fig. 3(c)). Interestingly, we observed microtubules distribute closely around the nucleus and formed a gradually widen channel, allowing the passage of mitochondria across the nucleus channels (magenta arrows in Fig. 3(c)). The results suggest that the mitochondria gathered to perinuclear region along microtubules, in order to support a large amount of energy consumption in the nucleus. In addition, PK Mito
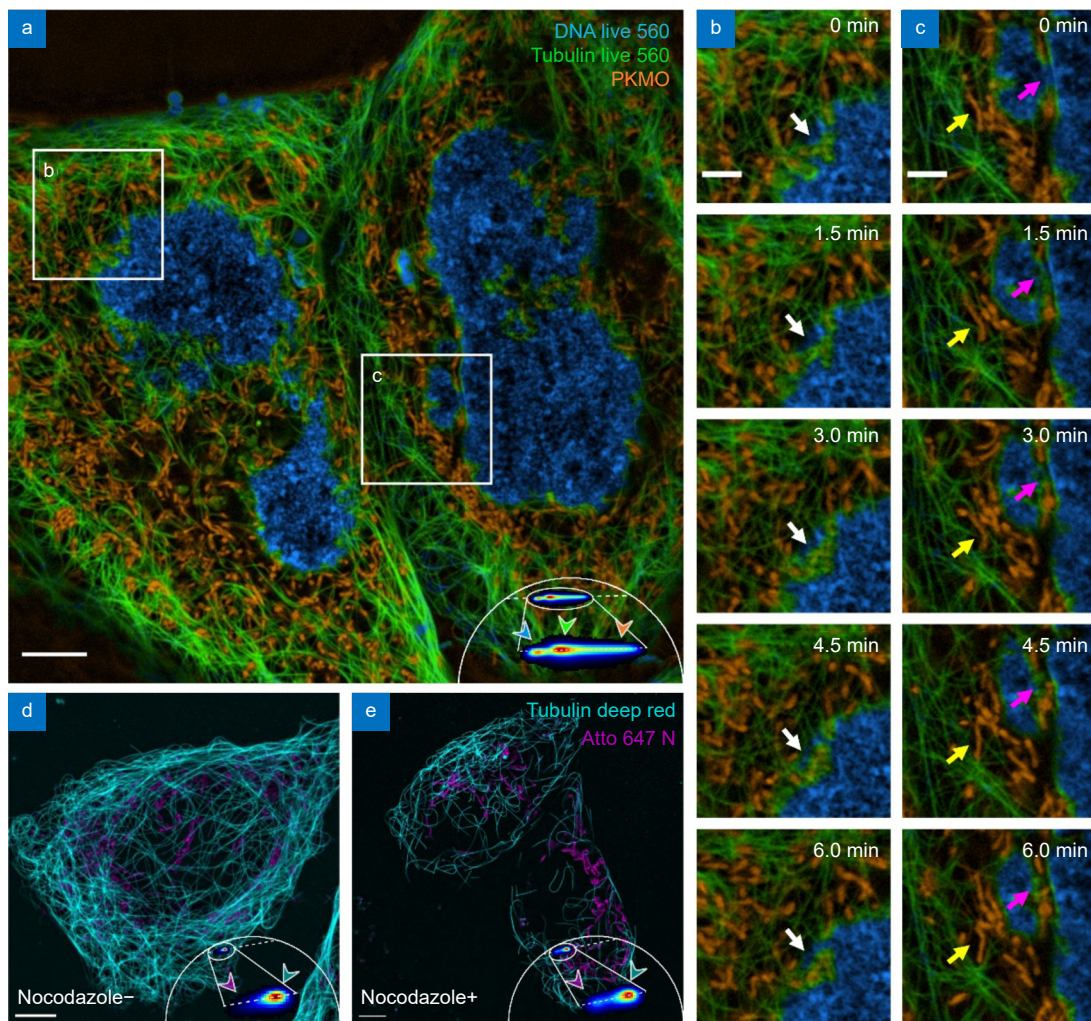
Fig. 3 | Multi-color live-cell mSTED using a single excitation beam. (**a**) Three-color imaging result of mSTED. Live U2OS cells were labeled with DNA Live 560 (blue; DNA), Tubulin Live 560 (green; microtubules), and PK Mito Orange (orange; mitochondria). (**b**, **c**) Cellular activity in the regions marked by the white boxes in (a). (**d**, **e**) Live U2OS cells were labeled with Tubulin Deep Red (cyan; microtubules) and Atto 647N (magenta; mitochondria) and imaged with mSTED (d) before and (e) after the addition of nocodazole. Scale bars: (a, d, e) 5 μm; (b, c) 2 μm.

Orange is able to stain mitochondrial cristae as shown in Supplementary information Fig. S10 using COS-7 cells. We also explored the possibility of 4-color mSTED imaging using a single excitation beam (Supplementary information Fig. S6). The results suggest the potential of mSTED to segment more structures using the minimum amount of excitation laser.

We further test and verify the performance of mSTED in live-cell after drug treatment (Fig. 3(d) and 3(e)). Nocodazole is a benzimidazole derivative widely used to study microtubule-dependent processes because of its ability to rapidly depolymerize microtubules[2,40]. After the addition of nocodazole, the number of microtubules was significantly reduced due to the depolymerization, and the cells presented a certain degree of shrinkage. No-

tably, the separation of microtubules and mitochondria was still workable after the addition of the drug, and most mitochondria still tend to remain around the existing microtubules according to our results (Fig. 3(e)). These results indicate that mSTED is still applicable to the study of the interactions between subcellular structures in live-cell even after the physiological state has changed.

Long-term multi-color live-cell mSTED based on both fluorescence lifetime and spectral identities

To observe and study the dynamics and interactions of more organelles in live-cell at the same time, we tried to investigate the upper limit of imaging channel numbers in live-cell mSTED by using both fluorescence lifetime

and spectral identities of the fluorescent probes. Although there is no theoretical limit to mSTED imaging channels, it is challenging to screen out proper fluorescent probe combinations which meet the following requirements at the same time: live-cell compatibility, adequate

brightness and anti-bleaching property for STED imaging, enough fluorescence lifetime differences between each other. Our results indicate the realization of five-color mSTED imaging of living U2OS cells stained with the following commercially available fluorescent probes:
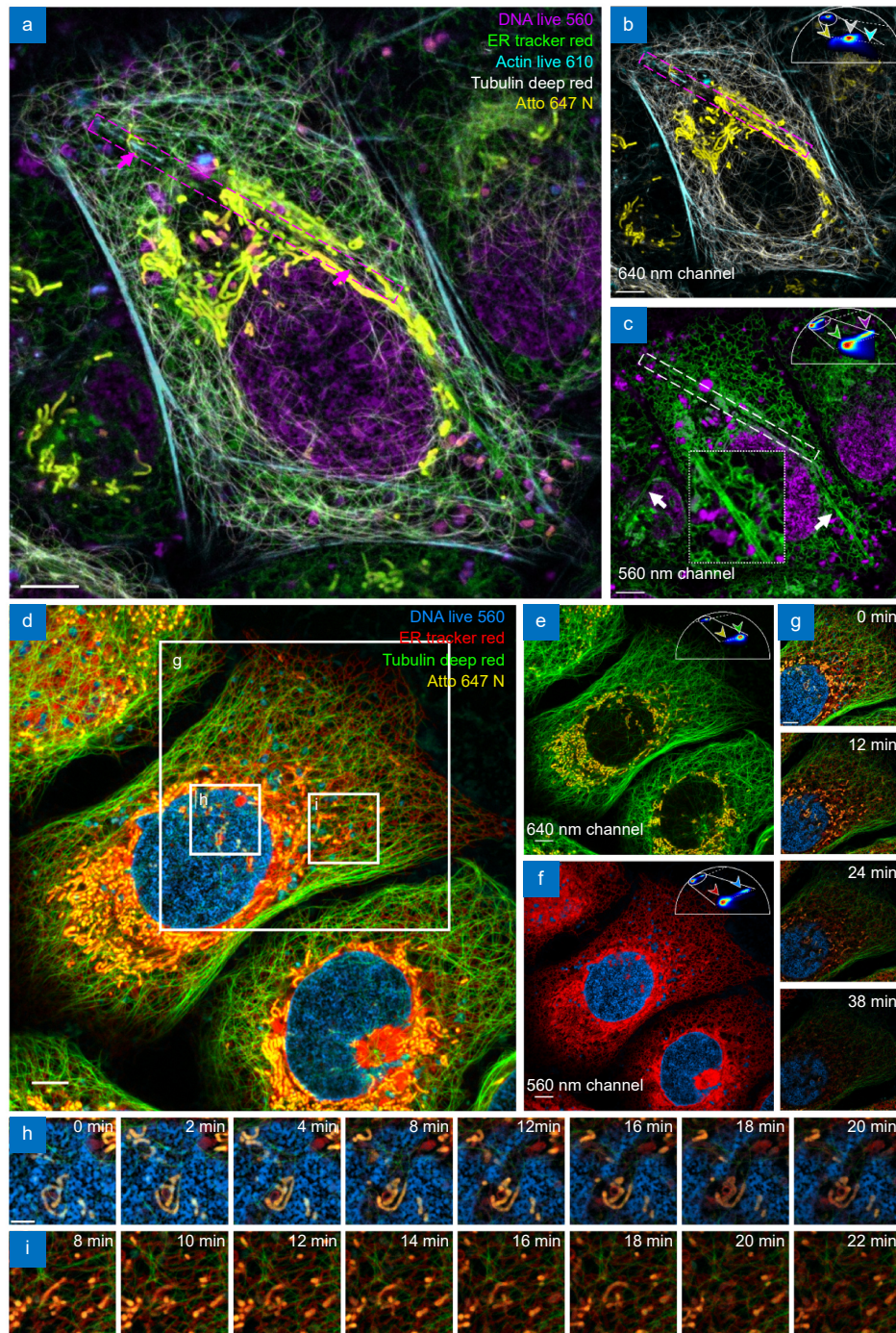

Fig. 4 | Extending mSTED through both spectra and fluorescence lifetime property separation. (**a–c**) Five-color live-cell mSTED imaging of live U2OS cells stained with DNA Live 560 (magenta; DNA), ER Tracker Red (green; Endoplasmic reticulum), Atto 647N (yellow; mitochondria), Tubulin Deep Red (white; microtubules), and Actin Live 610 (cyan; F-actin). (**d–f**) Four-color live-cell imaging results, Images of fluorescent probes excited at (**b**, **e**) 640-nm and (**c**, **f**) 560-nm laser wavelength. (**g-i**) Cellular activity in the boxed regions in (d) over a 38-minute period, with (**h**) and (**i**) demonstrating the interaction of multiple structures at different time points. Scale bars: (a–g) 5 μm; (h, i) 2 μm.

DNA Live 560 and ER Tracker Red in 560-nm excitation channel and Tubulin Deep Red, Atto 647N, and Actin Live 610 in 640-nm excitation channel (Fig. 4(a–c) and Fig. S2). Interestingly, a hollow structure of the endoplasmic reticulum (ER) signal with a length of over 20 μm was observed (dashed boxes in Fig. 4(a–c)). A portion of F-actin and microtubules colocalized with this hollow structure, and mitochondria seemed to distribute around this hollow as the ER did. Contrastively, our results showed another type of ER tubes with evident membrane boundary (white arrows in Fig. 4(c)). We measured the width of this tube (~400 nm) and it is much bigger than the conventional ER tubules width (~100 nm)[41]. These results indicate new formations of long-range transport of substances within the ER and the cytoplasm.

We then captured the dynamics and interactions of four subcellular structures in living U2OS cells in long-term mSTED imaging, by using two pairs of excitation-depletion laser beams (Fig. 4(d–i)). After imaging for 38 minutes, the morphology of the subcellular structures faded out due to both the photo-bleaching effect of fluorescence signal and the shrinkage of the living cell. The large enough information of long-term multi-color mSTED allowed us to discover interesting phenomena in cell biology. As an illustration, microtubules hold up some space beneath the nucleus for other organelles to move around (yellow dashed boxes in Fig. 4(h)), and mitochondrial fission (red arrows in Fig. 4(h)) and fusion (magenta arrows in Fig. 4(h)) happened in this limited space under the cooperation of ER and microtubules. In the peripheral cytoplasm, frequent deformation, fission, and fusion of ER (cyan dashed boxes in Fig. 4(h)) and mitochondria movement along microtubules and ER were observed during the long-term imaging (white arrows in Fig. 4(h, i)). These results highlight the superiority of multi-color mSTED in long-term live-cell imaging of multiple structures, enabling the systematical interpretation of organelle interaction network at the same time.

Conclusions

STED is widely used in studying subcellular structures, but its multicolor imaging capability is limited by labeling and spectroscopy, leading to significant difficulties and costs. In this work, we present a method for nanoscale live-cell multi-color imaging called mSTED. this method takes advantage of the differences in fluorescence lifetimes between a selected series of fluorescent probes to achieve segmentation between different structures based on phasor analysis. mSTED reduces photobleaching compared to spectral multiplexing, enabling long-term imaging of living cells. We have accomplished super-resolution imaging of up to five structures using mSTED, observing the activities and interactions of multiple organelles. Although alterations in the cellular state and microenvironment may affect the fluorescence lifetime of the probes and thus introduce increased crosstalk between structures, we have shown that our method is compatible with drug treatment and thus has broad application potential. mSTED can also be used in combination with other imaging tools, such as analyzing fluorescence anisotropy in homo-FRET in conjunction with nanoscale structures. We believe that mSTED will be further developed as more live-cell fluorescent probes for STED and more robust phase analysis algorithms are proposed.

In conclusion, our research extends STED to multicolor live-cell imaging, proposes a new avenue to study the complex and delicate interactome of intracellular organelles, and holds great promise for uncovering new biological discoveries.

References

1. Dong DS, Huang XS, Li LJ et al. Super-resolution fluorescence-assisted diffraction computational tomography reveals the three-dimensional landscape of the cellular organelle interactome. *Light Sci Appl* **9**, 11 (2020).
2. Valm AM, Cohen S, Legant WR et al. Applying systems-level spectral imaging and analysis to reveal the organelle interactome. *Nature* **546**, 162–167 (2017).
3. Abbe E. Beiträge zur Theorie des Mikroskops und der mikroskopischen Wahrnehmung. *Archiv Mikrosk Anatom* **9**, 413–468 (1873).
4. Hell SW, Wichmann J. Breaking the diffraction resolution limit by stimulated emission: stimulated-emission-depletion fluorescence microscopy. *Opt Lett* **19**, 780–782 (1994).
5. Gustafsson MGL. Surpassing the lateral resolution limit by a factor of two using structured illumination microscopy. *J Microsc* **198**, 82–87 (2000).
6. Klar TA, Jakobs S, Dyba M et al. Fluorescence microscopy with diffraction resolution barrier broken by stimulated emission. *Proc Natl Acad Sci USA* **97**, 8206–8210 (2000).
7. Betzig E, Patterson GH, Sougrat R et al. Imaging intracellular fluorescent proteins at nanometer resolution. *Science* **313**, 1642–1645 (2006).
8. Rust MJ, Bates M, Zhuang XW. Sub-diffraction-limit imaging by stochastic optical reconstruction microscopy (STORM). *Nat Methods* **3**, 793–796 (2006).
9. Huang B, Wang WQ, Bates M et al. Three-dimensional super-resolution imaging by stochastic optical reconstruction microscopy. *Science* **319**, 810–813 (2008).
10. Shroff H, Galbraith CG, Galbraith JA et al. Live-cell photoactivated localization microscopy of nanoscale adhesion dynamics.

    Nat Methods **5**, 417–423 (2008).
11. Müller CB, Enderlein J. Image scanning microscopy. *Phys Rev Lett* **104**, 198101 (2010).
12. Li CK, Le V, Wang XN et al. Resolution enhancement and background suppression in optical super-resolution imaging for biological applications. *Laser Photon Rev* **15**, 1900084 (2021).
13. Gould TJ, Schroeder LK, Pellett PA et al. STED microscopy. In Kubitscheck U. *Fluorescence Microscopy* (Wiley-VCH Verlag GmbH & Co. KGaA, Weinheim, 2017).
14. Müller T, Schumann C, Kraegeloh A. STED microscopy and its applications: new insights into cellular processes on the nanoscale. *ChemPhysChem* **13**, 1986–2000 (2012).
15. Vicidomini G, Bianchini P, Diaspro A. STED super-resolved microscopy. *Nat Methods* **15**, 173–182 (2018).
16. Hebisch E, Wagner E, Westphal V et al. A protocol for registration and correction of multicolour STED superresolution images. *J Microsc* **267**, 160–175 (2017).
17. Mehedi M, Smelkinson M, Kabat J et al. Multicolor stimulated emission depletion (STED) microscopy to generate high-resolution images of respiratory syncytial virus particles and infected cells. *Bio-Protocol* **7**, e2543 (2017).
18. Winter FR, Loidolt M, Westphal V et al. Multicolour nanoscopy of fixed and living cells with a single STED beam and hyperspectral detection. *Sci Rep* **7**, 46492 (2017).
19. Pellett PA, Sun XL, Gould TJ et al. Two-color STED microscopy in living cells. *Biomed Opt Express* **2**, 2364–2371 (2011).
20. Bottanelli F, Kromann EB, Allgeyer ES et al. Two-colour live-cell nanoscale imaging of intracellular targets. *Nat Commun* **7**, 10778 (2016).
21. Sidenstein SC, D'Este E, Böhm MJ et al. Multicolour multilevel STED nanoscopy of actin/spectrin organization at synapses. *Sci Rep* **6**, 26725 (2016).
22. Tonnesen J, Nadrigny F, Willig KI et al. Two-color STED microscopy of living synapses using a single laser-beam pair. *Biophys J* **101**, 2545–2552 (2011).
23. Spahn C, Grimm JB, Lavis LD et al. Whole-cell, 3D, and multicolor STED imaging with exchangeable fluorophores. *Nano Lett* **19**, 500–505 (2019).
24. Willig KI, Wegner W, Müller A et al. Multi-label *in vivo* STED microscopy by parallelized switching of reversibly switchable fluorescent proteins. *Cell Rep* **35**, 109192 (2021).
25. Chang CW, Sud D, Mycek MA. Fluorescence lifetime imaging microscopy. *Methods Cell Biol* **81**, 495–524 (2007).
26. Liu ZY, Pouli D, Alonzo CA et al. Mapping metabolic changes by noninvasive, multiparametric, high-resolution imaging using endogenous contrast. *Sci Adv* **4**, eaap9302 (2018).
27. Datta R, Gillette A, Stefely M et al. Recent innovations in fluorescence lifetime imaging microscopy for biology and medicine. *J Biomed Opt* **26**, 070603 (2021).
28. Bückers J, Wildanger D, Vicidomini G et al. Simultaneous multi-lifetime multi-color STED imaging for colocalization analyses. *Opt Express* **19**, 3130–3143 (2011).
29. Niehörster T, Löschberger A, Gregor I et al. Multi-target spectrally resolved fluorescence lifetime imaging microscopy. *Nat Methods* **13**, 257–262 (2016).
30. Ranjit S, Malacrida L, Jameson DM et al. Fit-free analysis of fluorescence lifetime imaging data using the phasor approach. *Nat Protoc* **13**, 1979–2004 (2018).
31. Digman MA, Caiolfa VR, Zamai M et al. The phasor approach to fluorescence lifetime imaging analysis. *Biophys J* **94**, L14–L16 (2008).
32. Torrado B, Malacrida L, Ranjit S. Linear combination properties of the phasor space in fluorescence imaging. *Sensors* **22**, 999 (2022).
33. Shi W, Koo DES, Kitano M et al. Pre-processing visualization of hyperspectral fluorescent data with spectrally encoded enhanced representations. *Nat Commun* **11**, 726 (2020).
34. Scipioni L, Rossetta A, Tedeschi G et al. Phasor S-FLIM: a new paradigm for fast and robust spectral fluorescence lifetime imaging. *Nat Methods* **18**, 542–550 (2021).
35. Frei MS, Koch B, Hiblot J et al. Live-cell fluorescence lifetime multiplexing using synthetic fluorescent probes. *ACS Chem Biol* **17**, 1321–1327 (2022).
36. Frei MS, Tarnawski M, Roberti MJ et al. Engineered HaloTag variants for fluorescence lifetime multiplexing. *Nat Methods* **19**, 65–70 (2022).
37. Gonzalez Pisfil M, Nadelson I et al. Stimulated emission depletion microscopy with a single depletion laser using five fluorochromes and fluorescence lifetime phasor separation. *Sci Rep* **12**, 14027 (2022).
38. Battisti A, Digman MA, Gratton E et al. Intracellular pH measurements made simple by fluorescent protein probes and the phasor approach to fluorescence lifetime imaging. *Chem Commun* **48**, 5127–5129 (2012).
39. Shim SH, Xia CL, Zhong GS et al. Super-resolution fluorescence imaging of organelles in live cells with photoswitchable membrane probes. *Proc Natl Acad Sci USA* **109**, 13978–13983 (2012).
40. Vasquez RJ, Howell B, Yvon AM et al. Nanomolar concentrations of nocodazole alter microtubule dynamic instability in vivo and in vitro. *Mol Biol Cell* **8**, 973–985 (1997).
41. Zhang YD, Schroeder LK, Lessard MD et al. Nanoscale subcellular architecture revealed by multicolor three-dimensional salvaged fluorescence imaging. *Nat Methods* **17**, 225–231 (2020).

Acknowledgements

Author contributions

Conceived and oversaw the project: Y. B. Han, C. F. Kuang, Z. M. Zhang. Initiated the designs for microscope: C. F. Kuang. Initiated the designs for biological experiments: Y. B. Han. Designed and developed the microscope: Z. M. Zhang, Y. R. Huang, L. Xu. Designed the imaging software: Z. M. Zhang. Designed the processing algorithm: Y. R. Huang, Z. M. Zhang. Prepared the experimental samples: W. L. Tao, W. W. Gong. Synthesized the fluorescent probes: Y. F. Wei. Performed the experiments: Y. R. Huang, W. L. Tao. All authors inspected data and contributed to the drafting of the manuscript. Supervised research: Z. M. Zhang, Y. B. Han, C. F. Kuang, X. Liu. Directed research: Y. B. Han.

Competing interests

The authors declare no competing financial interests.

Supplementary information

Supplementary information for this paper is available at
https://doi.org/10.29026/oea.2024.240035